A spectrokinetic study of CH2I and CH2IO2 radicals

ARTICLE *in* INTERNATIONAL JOURNAL OF CHEMICAL KINETICS · FEBRUARY 1994

Impact Factor: 1.52 · DOI: 10.1002/kin.550260204

A Spectrokinetic Study of CH_2I and CH_2IO_2 Radicals

JENS SEHESTED, THOMAS ELLERMANN, and OLE JOHN NIELSEN*
Chemical Reactivity Section, Environmental Science and Technology Department, Risø National Laboratory, DK-4000 Roskilde, Denmark

Abstract

The UV absorption spectrum and kinetics of CH_2I and CH_2IO_2 radicals have been studied in the gas-phase at 295 K using a pulse radiolysis UV absorption spectroscopic technique. UV absorption spectra of CH_2I and CH_2IO_2 radicals were quantified in the range 220–400 nm. The spectrum of CH_2I has absorption maxima at 280 nm and 337.5 nm. The absorption cross-section for the CH_2I radicals at 337.5 nm was $(4.1 \pm 0.9) \times 10^{-18}$ cm^2 molecule^{-1}. The UV spectrum of CH_2IO_2 radicals is broad. The absorption cross-section at 370 nm was $(2.1 \pm 0.5) \times 10^{-18}$ cm^2 molecule^{-1}. The rate constant for the self reaction of CH_2I radicals, $k = 4 \times 10^{-11}$ cm^3 molecule^{-1} s^{-1} at 1000 mbar total pressure of SF_6, was derived by kinetic modelling of experimental absorbance transients. The observed self-reaction rate constant for CH_2IO_2 radicals was estimated also by modelling to $k = 9 \times 10^{-11}$ cm^3 molecule^{-1} s^{-1}. As part of this work a rate constant of $(2.0 \pm 0.3) \times 10^{-10}$ cm^3 molecule^{-1} s^{-1} was measured for the reaction of F atoms with CH_3I. The branching ratios of this reaction for abstraction of an I atom and a H atom were determined to (64 ± 6)% and (36 ± 6)%, respectively.

Introduction

Understanding of the kinetics and spectroscopy of alkyl peroxy radicals has long been recognized as important due to the central role peroxy radicals play in the degradation of volatile organic compounds in the troposphere. Comprehensive knowledge has been achieved about several series of alkyl-, haloalkyl-, acyl-, oxygen substituted-, and unsaturated peroxy radicals [1,2]. The halogenated alkyl peroxy radicals have received special interest due to the importance of chlorine and bromine atoms in the degradation of stratospheric ozone, and a number of these have previously been studied in our laboratory [3,4]. Of the monohalogenated methylperoxy radicals the fluorine [3], chlorine [5], and bromine [4] species have been studied so far. The objective of this work was to study iodine methylperoxy radicals.

Iodine methylperoxy radicals have to the authors knowledge not been studied so far, probably because they are of limited importance from an atmospheric viewpoint. This is in spite of the natural production of CH_3I in the marine boundary layer. Methyl iodide has a broad UV absorption spectrum with a maximum at 260 nm which extends into the UVA and UVB spectral regions. The photolysis lifetime for CH_3I is about 8 h [6] making photolytic cleavage the primary degradation channel for CH_3I in the atmosphere:

$$(1) \qquad CH_3I + h\nu \longrightarrow CH_3 + I$$

*To whom correspondence should be addressed.

International Journal of Chemical Kinetics, Vol. 26, 259–272 (1994)
 CCC 0538-8066/94/020259-14

Another important degradation channel in the troposphere is reaction with OH:

(2a) $$CH_3I + OH \longrightarrow CH_2I + H_2O$$

(2b) $$\longrightarrow CH_3 + HOI$$

The overall rate constant for the reaction between CH_3I and OH has been determined by Wayne and co-workers [7]. The overall rate constant for reaction (2) was determined to $(7.2 \pm 0.7) \times 10^{-14}$ cm^3 molecule^{-1} s^{-1} [7]. Wayne and co-workers [7] estimated from an average OH concentration in the atmosphere of $(7.7-50) \times 10^5$ cm^{-3} that only 2–11% of the atmospheric CH_3I content is consumed via reaction (2). The product distribution of the reaction of OH radicals with CH_3I has not yet been determined. However, under the assumption that CH_3I is removed from the atmosphere only by photolysis and reaction with OH, an upper limit of the CH_2I formation can be estimated to 11% of the consumed CH_3I.

Other possible minor loss mechanisms for CH_3I in the atmosphere includes reaction with Cl atoms and NO_3 radicals. The reaction of CH_3I with NO_3 is slow, $k = 3.4 \times 10^{-17}$ cm^3 molecule^{-1} s^{-1} [8], and this reaction is therefore unimportant in the atmosphere. The rate constant for reaction of Cl atoms with CH_3I is not known. However, it is interesting to note that both the CH_3I and the Cl atom concentrations are high in the marine environment. This tends to increase the importance of the reaction of CH_3I with Cl atoms but it is unlikely that this reaction can compete with photolysis of CH_3I in the atmosphere.

CH_2IO_2 radicals are formed by the reaction of CH_2I radicals with O_2:

(3) $$CH_2I + O_2 + M \longrightarrow CH_2IO_2 + M$$

Although of minor importance in the atmosphere CH_2IO_2 is interesting in order to understand the effect of halogen substitution on the spectrum and kinetics of peroxy radicals. The fluoro and chloro methylperoxy radicals have common spectroscopic and kinetic properties. However, the bromo methylperoxy radical has an UV spectrum with a different shape and significantly higher absorption cross-sections than most other peroxy radicals [4]. Also the apparent rate constant for the peroxy radical self reaction is considerably higher for the CH_2BrO_2 radical than observed for the CH_2FO_2 and CH_2ClO_2 radicals. To extend the information on the kinetic and spectroscopic data for the homolog series of monohalogenated methylperoxy radicals, we have carried out a study of the iodine methylperoxy radical. The results are reported here together with spectroscopic and kinetic data of the CH_2I radical.

Experimental

A pulse radiolysis transient UV absorption setup was used to study the UV absorption spectra of CH_2I and CH_2IO_2 radicals. The experimental system has been described in detail elsewhere [9–11] and will only be briefly discussed here.

CH_2I radicals were produced by pulse radiolysis of CH_3I/SF_6 gas mixtures in a one liter stainless steel reactor with a 30 ns pulse of 2 MeV electrons from a 705B Febetron accelerator. The irradiation dose, given relative to full dose herein, was varied by stainless steel attenuators. SF_6 in great excess was used to produce fluorine atoms. Radiolysis of gas mixtures of 1 mbar of CH_3I and 1000 mbar SF_6 leads to production of CH_2I and CH_3 radicals by the following reactions:

(4) $SF_6 + 2\ MeV\ e^- \longrightarrow F + products$

(5a) $F + CH_3I \longrightarrow HF + CH_2I$

(5b) $F + CH_3I \longrightarrow IF + CH_3$

When 40 mbar O_2 was added to the reaction mixture, CH_2IO_2 and CH_3O_2 radicals were produced by addition of O_2 to CH_2I and CH_3, respectively:

(3) $CH_2I + O_2 + M \longrightarrow CH_2IO_2 + M$

(6) $CH_3 + O_2 + M \longrightarrow CH_3O_2 + M$

The analyzing light was provided by a pulsed 150 W Xenon lamp. Internal White type optics gave total optical pathlengths of 40, 80, and 120 cm. The light beam was detected by a 1 m Hilger and Watts grating monochromator operated at a spectral resolution of 0.8 nm, linked to a Hamamatsu R928 photomultiplyer and a Biomation 8100 transient digitizer. A PDP11 computer controlled the data handling and storage of the data. All transients used in this work are single pulse transients, no signal averaging was used.

Reagents used were: SF_6, 959–1000 mbar, delivered by Gerling and Holz (> 99.9%); Ultra high purity O_2, 0–40 mbar, supplied by L'Air Liquide; CH_4, 5 mbar, received from Gerling and Holz (> 99%); CH_3I, 0.3–1 mbar, obtained from Merck-Schuchardt at a stated purity of > 99%. Volatile impurities were removed from CH_3I by freeze–pump–thaw cycles. SF_6, CH_4, and O_2 were used as received.

The uncertainties reported in this article are 2σ values unless otherwise stated. Normal statistical error propagation is used to calculate combined uncertainties.

Results

Examples of absorption transients obtained by radiolysis of gas mixtures of 1 mbar CH_3I and 1000 mbar SF_6 recorded at different wavelengths are shown in Figure 1. The different transients reflect that the fluorine atoms, produced by radiolysis of SF_6, both abstract iodine and hydrogen atoms from CH_3I:

(5a) $F + CH_3I \longrightarrow HF + CH_2I$

(5b) $F + CH_3I \longrightarrow IF + CH_3$

The formation and decay of the methyl radicals can be observed at 216.4 nm, where these radicals absorb strongly. The absorbance at 370 nm and 470.2 nm can, as discussed below, be ascribed to the formation and decay of CH_2I radicals and IF molecules, respectively. When O_2 is added to the reaction mixture the kinetics and the observed absorbance change. We attribute this change to the formation of CH_2IO_2 and CH_3O_2 via reaction (3) and (6).

Rate Constant and Branching Ratio for Reaction (5)

Determination of absolute concentrations of product radicals produced from reaction of F atoms with CH_3I requires knowledge of the initial fluorine atom yield. This is achieved by measurements of the yield of CH_3 radicals formed by radiolysis of

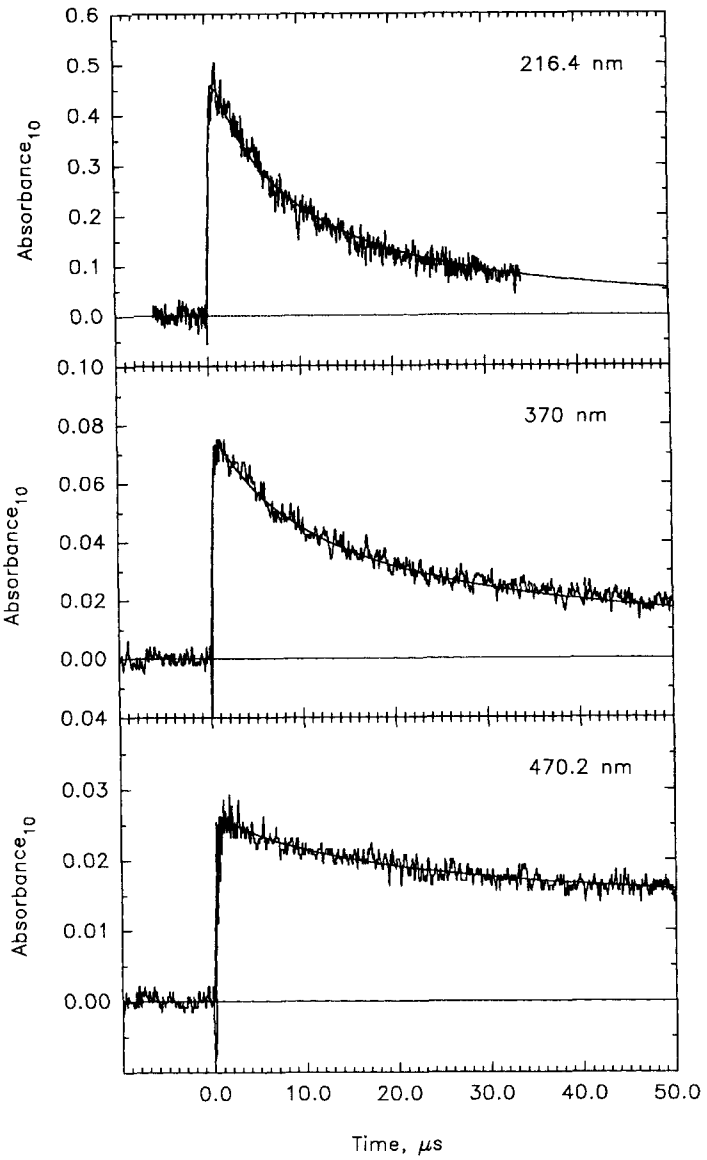

Figure 1. The transient UV absorption at 216.4 nm, 370 nm, and 470.2 nm following pulse radiolysis of mixtures of 1 mbar CH_3I and 1000 mbar SF_6. Solid lines are fit to the observed data, see text.

SF_6/CH_4 mixtures by the following reactions:

(4) $$SF_6 + e^- \longrightarrow F + \text{products}$$

(7) $$F + CH_4 \longrightarrow CH_3 + HF$$

Figure 2 shows the absorption at 216.4 nm as a function of the relative dose produced by radiolysis of 1 mbar CH_4 and 1000 mbar SF_6. A least-squares analysis of the data in Figure 2 gives a slope of 2.14 ± 0.13. The absorption cross-section of CH_3

radicals at 216.4 nm is 4.12×10^{-17} cm^2 molecule^{-1} [12]. From this absorption cross-section and the slope obtained from Figure 2 an initial fluorine atom concentration of $(3.0 \pm 0.4) \times 10^{15}$ molecules cm^{-3} was obtained. The uncertainty includes an estimated uncertainty of 10% on σ_{CH3} (216.4 nm) and the uncertainty on the slope in Figure 2.

The reaction between fluorine atoms and CH_3I proceeds through two channels [13]:

(5a) $$F + CH_3I \longrightarrow CH_3 + IF$$

(5b) $$\longrightarrow CH_2I + HF$$

Wörsdörfer and Heydtmann [13] have studied reaction (5) and derived $k_5 = (1.7 \pm 0.3) \times 10^{-10}$ cm^3 molecule^{-1} s^{-1}. In addition they report the branching ratio of channel (a) and (b) to be (62 ± 8)% and (38 ± 8)%, respectively. This mechanism was checked in our system. The following two sets of experiments were performed: First, determination of the yield of CH_3 radicals by detection of the absorbance at 216.4 nm and second, measurements between 450 and 500 nm of the formation of IF molecules.

The absorbance at 216.4 nm following pulse radiolysis of 1000 mbar SF_6 and 1 mbar CH_3I is plotted as a function of dose in Figure 2. It is evident from the figure that the absorbance is proportional to the irradiation dose at least up to one third of the maximum dose. A linear least-squares fit of the data gives a slope of 1.42 ± 0.07. By comparing this absorption with the absorption obtained in the CH_4/SF_6 system we can determine the branching ratio in reaction (5). However, since the absorption in the CH_3I/SF_6 system at 216.4 nm is due to both CH_3 and CH_2I radicals a small correction needs to be made. To estimate the absorbance due to CH_2I radicals at 216.4 nm, the maximum absorbance was measured at 217.4 nm following pulse radiolysis of CH_4/SF_6 and CH_3I/SF_6 mixtures, respectively. The results were 0.195 and 0.144 using a dose of 0.32 and a pathlength of 40 cm. The CH_3 peak at 216.4 nm is sharp. The absorbance at 217.4 nm in the CH_4/SF_6 system was 3.3 times less than that at 216.4 nm. If we then assume that CH_2I radicals have similar absorption cross-sections at 216.4 nm and 217.4 nm, it is possible to correct the absorption at 216.4 nm for the CH_2I contribution. This is presumably a valid assumption since as seen in Figure 5 the absorption cross-section of CH_2I derived below does not change much

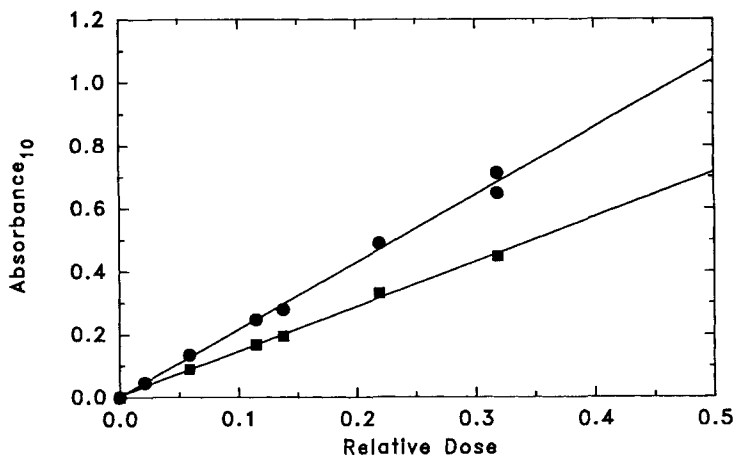

Figure 2. Maximum transient absorptions at 216.4 nm following pulse radiolysis of a CH_4/SF_6 mixture (●) and a CH_3I/SF_6 mixture (■) plotted as a function of the dose.

between 220 and 250 nm. From the data and the assumption made above we calculate that the CH_2I absorbance at 216.4 nm in the CH_3I/SF_6 system is 0.05. There is substantial uncertainty on this value (we estimate 100%). However, the correction is small compared to the overall absorption, (1.42 ± 0.07). Thus the absorption due to CH_2I radicals at 216.4 nm in the CH_3I/SF_6 system is (1.37 ± 0.09).

This absorption can be used to calculate the methyl yield in the CH_3I/SF_6 system. By comparing the obtained methyl absorbance with the absorbance at 216.4 nm in the SF_6/CH_4 system (2.14 ± 0.13), we determine the methyl yield in the SF_6/CH_3I system to be (64 ± 6)% and the CH_2I yield to be (36 ± 6)%. These values are in excellent agreement with those of Wörsdörfer and Heydtmanns [13] given above.

As an additional check of the mechanism of the reaction of fluorine atoms with CH_3I, we performed measurements of IF. Previous results [14–16] indicate that IF absorbs between 420 and 600 nm. The spectrum is a line spectrum. In agreement with Clark and Littlewood [14] we detect absorption peaks at 462.5 nm, 470.2 nm, and 478.4 nm. The measured absorbances are 0.062, 0.076, and 0.074, when 1 mbar CH_3I, 1000 mbar SF_6, analyzing path-length of 120 cm, and maximum dose was employed. The absorbance at 460 nm, where the absorption of IF is small, is 0.008. Our observations show, that IF was indeed produced in this chemical system. To our knowledge no absorption cross-sections have been published for IF so it was not possible to quantify the IF yield. However, the IF transients contain information about the rate constant of reaction (5):

(5) $$F + CH_3I \longrightarrow \text{products}$$

The observed formation of IF can be fitted well by use of first-order kinetics. In Figure 3 the fitted pseudo-first-order rate constants for the formation of IF are plotted as a function of the CH_3I concentration. The slope gives (2.0 ± 0.3) × 10^{-10} cm^3 $molecule^{-1}$ s^{-1}. This rate constant is in good agreement with the literature value of (1.7 ± 0.3) × 10^{-10} cm^3 $molecule^{-1}$ s^{-1} [13].

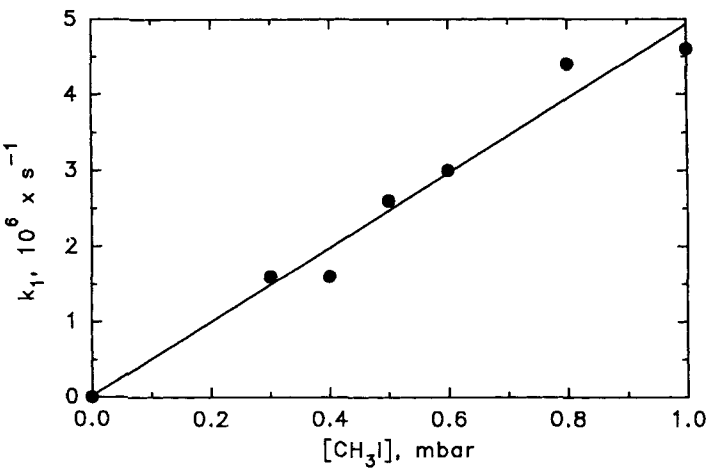

Figure 3. k_1 plotted as a function of [CH_3I]. k_1 was determined by a first-order fit of the IF transients at 470.2 nm. IF was formed by pulse radiolysis of mixtures of 1 mbar Ch_3I and 1000 mbar SF_6 at dose = 0.318. The line through the data points was formed by a regression analysis of the data.

CH_2I Spectrum

The absolute yield of the CH_2I radicals can be determined from the initial fluorine atom yield and the branching ratio of reaction (5), if all fluorine atoms react with CH_3I and secondary reactions are unimportant. Figure 4 shows the maximum absorbance at 337.5 nm due to CH_2I formation plotted as a function of irradiation dose. Gas mixtures of 1 mbar CH_3I and 1000 mbar SF_6 were used. It is evident from Figure 4, that the CH_2I absorbance is proportional to the dose at doses below 0.41. At higher doses which is equal to higher radical concentrations, the curve bends downwards. This can be explained by radical-radical reactions, which become increasingly important as the radical concentration is increased.

From a linear least-squares analysis of the data in Figure 4 up to dose 0.32 we obtain a slope of (0.231 ± 0.015). When combined with the absolute fluorine atom yield, (3.0 ± 0.4) × 10^{15} molecules cm^{-3}, and the branching ratio of reaction (5) for CH_2I production, (36 ± 6)%, we can calculate the absorption cross-section of CH_2I at 337.5 nm to (4.1 ± 0.9) × 10^{-18} cm^2 $molecule^{-1}$. The uncertainty on the absorption cross-section include the uncertainty on all three pieces of information used in the calculation.

To map out the spectrum of CH_2I the maximum transient absorbance at the above mentioned conditions is determined in the range wavelength 220–400 nm. We assign this spectrum to CH_2I, because IF and HF do not absorb in this wavelength region. A correction had to be made for the decrease of absorbance due to loss of CH_3I. This loss equals the fluorine atom yield and the correction could then be carried out by use of CH_3I absorption cross-sections reported by Porret and Goodeve [17]. Finally, the absolute spectrum of CH_2I was obtained by scaling the initial absorptions to that at 337.5 nm. In Figure 5 the obtained CH_2I spectrum is shown, and absorption cross-sections are listed in Table I.

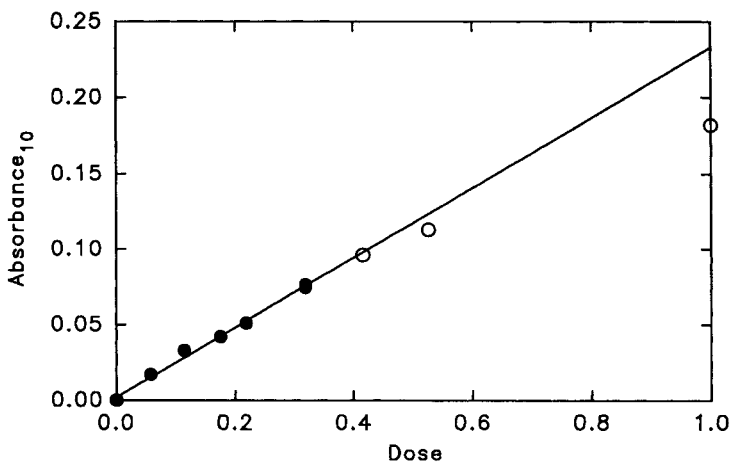

Figure 4. Maximum transient absorption at 337.5 nm following pulse radiolysis of mixtures of 1 mbar CH_3I and 1000 mbar SF_6 as function of dose. The straight line on the plot was found by linear regression analysis of the data up to dose 0.32.

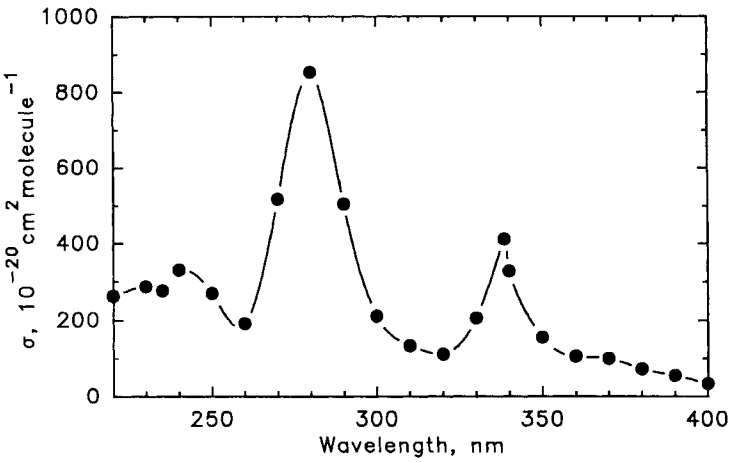

Figure 5. UV absorption spectrum of CH_2I radicals.

Decay of CH_2I, IF, and CH_3

Examples of the decay of CH_2I, IF, and CH_3 are displayed in Figure 1. As shown in this figure the three species decay on the same time scale. When CH_2I and CH_3 have disappeared IF is still present and do not decay any further. We therefore assume that IF molecules are removed by reaction with CH_3 and CH_2I radicals. This assumption can be tested by use of O_2 molecules as a scavenger for CH_3 and CH_2I radicals. When 40 mbar of O_2 was added to the reaction mixture the IF absorption transients build up to a stable plateau and no sign of IF removal was detected. The observed behavior

TABLE I. Measured UV absorption cross-sections of the CH_2I and CH_3IO_2 radicals.

Wavelength (nm)	$10^{20}\sigma_{CH_3I}$ (cm^2 $molecule^{-1}$)	$10^{20}\sigma_{CH_3IO_2}$ (cm^2 $molecule^{-1}$)
220	262	726
230	287	604
235	276	–
240	330	573
250	270	399
260	191	355
270	517	300
280	852	–
290	504	–
300	211	252
310	133	241
320	111	240
330	205	257
338	411	–
340	327	257
350	155	254
360	105	229
370	100	211
380	72	182
390	56	139
400	33	114

of CH_2I, CH_3, and IF can be explained by the following set of reactions:

(8) $$CH_3 + CH_3 + M \longrightarrow CH_3CH_3 + M$$

(9) $$CH_3 + CH_2I + M \longrightarrow CH_3CH_2I + M$$

(10) $$CH_2I + CH_2I + M \longrightarrow CH_2ICH_2I + M$$

(11) $$CH_3 + IF \longrightarrow CH_3F + I$$

(12) $$CH_2I + IF \longrightarrow CH_2IF + I$$

This kinetic mechanism can qualitatively explain the observations of the behavior of the three transients in Figure 1. Quantitative results can only be obtained by making several assumptions since only one out of the five reactions in the proposed kinetic mechanism has been studied before. The literature values for the rate constant of reaction (8) are all close to 6×10^{-11} cm^3 $molecule^{-1}$ s^{-1} [18]. The suggested products of reaction (9) and (10) are found by analogy to reaction (8). Since the rate constant for $CH_2Cl + CH_2Cl$, $k = 2.8 \times 10^{-11}$ cm^3 $molecule^{-1}$ s^{-1} [19], and for $CH_2Br + CH_2Br$, $k = 2.9 \times 10^{-11}$ cm^3 $molecule^{-1}$ s^{-1} [4], are similar, we will as an initial guess use $k_{10} = 2.9 \times 10^{-11}$ cm^3 $molecule^{-1}$ s^{-1} and take k_9 as the arithmetic mean of reaction (8) and (10), 4.5×10^{-11} cm^3 $molecule^{-1}$ s^{-1}

Reaction (11) and (12) have not been studied before. The products of reaction (11) are presumably either CH_3F and I or CH_3I and F. Since the first reaction channel is 177 kJ mol^{-1} exothermic and the second 39 kJ mol^{-1} endothermic, we estimate the first channel to be dominant (thermodynamic data from Sugawara et al. [20]). By analogy it is assumed that the products of reaction (12) are CH_2IF and I.

To be able to simulate the three transients on Figure 1 a final assumption has to be made: $k_{11} = k_{12}$. Reactions (5) and (8)–(12) were used as the kinetic model to fit the three transients in Figure 1 by varying the parameter $\alpha = k_{11} = k_{12}$ and k_{10} and still keeping k_9 at the arithmetic mean of k_8 and k_{10}. We obtain a good fit (see Fig. 1) with $\alpha = k_{11} = k_{12} = 3 \times 10^{-11}$, $k_9 = 5 \times 10^{-11}$, and $k_{10} = 4 \times 10^{-11}$ cm^3 $molecule^{-1}$ s^{-1}.

Spectrum of CH_2IO_2

When oxygen is added to the reaction mixture the transient UV absorption changes. Part of the UV absorbance can be attributed to CH_3O_2 formed by:

(6) $$CH_3 + O_2 + M \longrightarrow CH_3O_2 + M$$

The CH_2IO_2 radical can be produced by addition of CH_2I radicals and molecular oxygen:

(3) $$CH_2I + O_2 + M \longrightarrow CH_2IO_2 + M$$

Production of CH_3O_2 can only partly account for the observed absorbance. We assign this additional absorption to the CH_2IO_2 radical. When O_2 is added to the reaction mixture a small amount of FO_2 is formed as an unwanted side product:

(13) $$F + O_2 + M \longrightarrow FO_2 + M$$

Since the rate constant of reaction (13), $(2.0 \pm 0.3) \times 10^{-13}$ in 1000 mbar SF_6 [21], and the spectrum of FO_2 [21] is known it is possible to correct for the absorption due to FO_2.

To ensure a stoichiometric conversion of fluorine atoms into CH_2IO_2, CH_3O_2, and FO_2 radicals the absorption as a function of the dose was measured at 370 nm (see

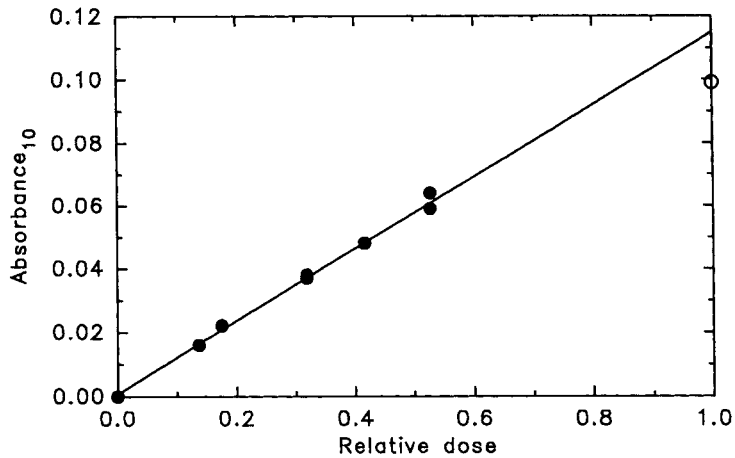

Figure 6. Maximum transient absorption at 370 nm following pulse radiolysis of mixtures of 1 mbar CH_3I, 40 mbar O_2, and 959 mbar SF_6 plotted as a function of the dose. The straight line was obtained by a linear least-squares analysis of the data up to dose 0.53.

Fig. 6). Gas mixtures of 1 mbar CH_3I, 40 mbar O_2, and 959 mbar SF_6 were used. The maximum absorbance was reached 2 μs after the electron pulse initiation. The absorption shown in Figure 6 is linear with dose up to dose 0.53. Using a dose of 0.53 or less ensures a stoichiometric conversion of F atoms into CH_3O_2, CH_2IO_2, and FO_2. The deviation from linearity at maximum dose is due to unwanted radical-radical reactions. At doses equal to or less than half dose these secondary reactions are negligible. A linear least-squares analysis of the low dose data gives a slope of (0.114 ± 0.006).

The absorption cross-section of CH_2IO_2 at 370 nm was calculated to (2.1 ± 0.5) × 10^{-18} cm^2 $molecule^{-1}$ by use of the following four pieces of information: (1) the fluorine atom yield at maximum dose and 1000 mbar SF_6, (3.0 ± 0.4) × 10^{15} molecules cm^{-3}; (2) the ratio of the fluorine atoms which react with CH_3I to give CH_2I as the product, (36 ± 6)%; (3) the slope of the straight line calculated from the data on Figure 6 up to half dose, 0.114 ± 0.006; and (4) the rate constant for the reaction between F atoms and O_2, k = (2.0 ± 0.3) × 10^{-13} cm^3 $molecules^{-1}$ s^{-1} [21]. The uncertainty on $\sigma(CH_2IO_2)$ was found by normal error propagation of the uncertainty on the four pieces of information used in the calculation.

To determine the absorption cross-sections of CH_2IO_2 between 220 nm and 400 nm the UV maximum absorbance following pulse radiolysis of $CH_3I/SF_6/O_2$ mixtures was measured for at least every 10 nm. At 280 nm and 290 nm product absorption made quantification of the CH_2IO_2 absorption impossible. 1 mbar CH_3I, 40 mbar O_2, 959 mbar SF_6, and half dose was used to ensure complete conversion of fluorine atoms into peroxy radicals. To avoid potential complications from the initial absorption due to CH_2I, the absorbance was measured 2 μs after the electron pulse. Corrections were made for the absorption due to CH_3O_2 [1] and FO_2 [21] radicals. In addition the disappearance of CH_3I had to be taken into account as discussed earlier. By scaling the absorbances to the absorption cross-section at 370 nm we obtain the UV absorption spectrum for CH_2IO_2 displayed in Figure 7 and listed in Table I.

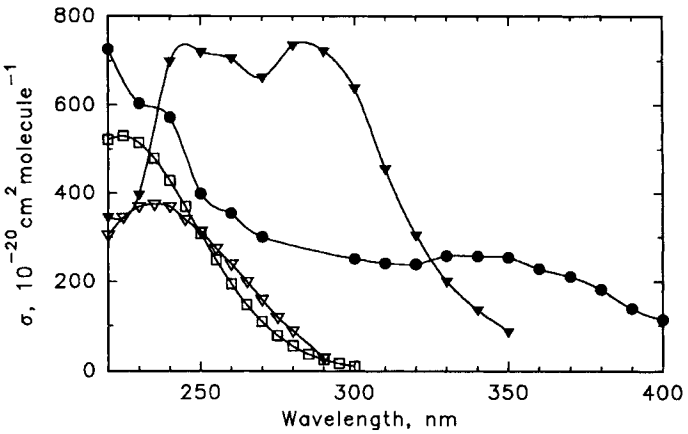

Figure 7. UV absorption spectrum of CH_2IO_2 (●) radicals compared with the spectra of CH_2FO_2 (□), CH_2ClO_2 (▽), and CH_2BrO_2 (▼) radicals.

Decay of CH_2IO_2 and CH_3O_2

Experimental traces from the pulse radiolysis of $CH_3I/O_2/SF_6$ mixtures taken at three different wavelengths are shown in Figure 8. At 370 nm the absorption rapidly decays to a plateau with a half-life of approximately 5 μs. On the same time scale the absorption transient at 300 nm increases to a stable plateau. At 230 nm, the absorption is almost constant after the formation of the peroxy radicals. At this wavelength only a small decrease in the absorption is seen between 10 and 40 μs. From these three transients it is possible to derive the approximate kinetic behavior of the CH_2IO_2 radicals while extraction of the kinetic behavior of the CH_3O_2 radicals from the data is impossible; at 300 nm one or more products dominate the observed absorption and at 230 nm the product absorption is so prominent that the decay of the CH_3O_2 radicals could not be observed.

The trace recorded at 370 nm shows the kinetics of CH_2IO_2 radical and a significant product absorption. The absorbance transient can not be fitted well by neither first-order nor by second-order kinetics. This can be explained by the self reactions and cross reaction of CH_2IO_2 and CH_3O_2 which lead to mixed kinetics:

(14) $$CH_2IO_2 + CH_2IO_2 \longrightarrow \text{Products}$$

(15) $$CH_2IO_2 + CH_3O_2 \longrightarrow \text{Products}$$

(16) $$CH_3O_2 + CH_3O_2 \longrightarrow \text{Products}$$

Another potential complication is secondary chemistry. Products of the CH_2IO_2 decay may react fast with CH_2IO_2 and thereby speed up the apparent decay of the CH_2IO_2 radicals. In addition secondary products might absorb at 370 nm, changing the observed decay half-life.

Even though the rate constants k_{14} and k_{15} can only be derived from our measurements by making several assumptions, two interesting facts should be noted. The decay of CH_2IO_2 radicals is fast ($t_{1/2}$ = 5 μs at half dose) compared with other

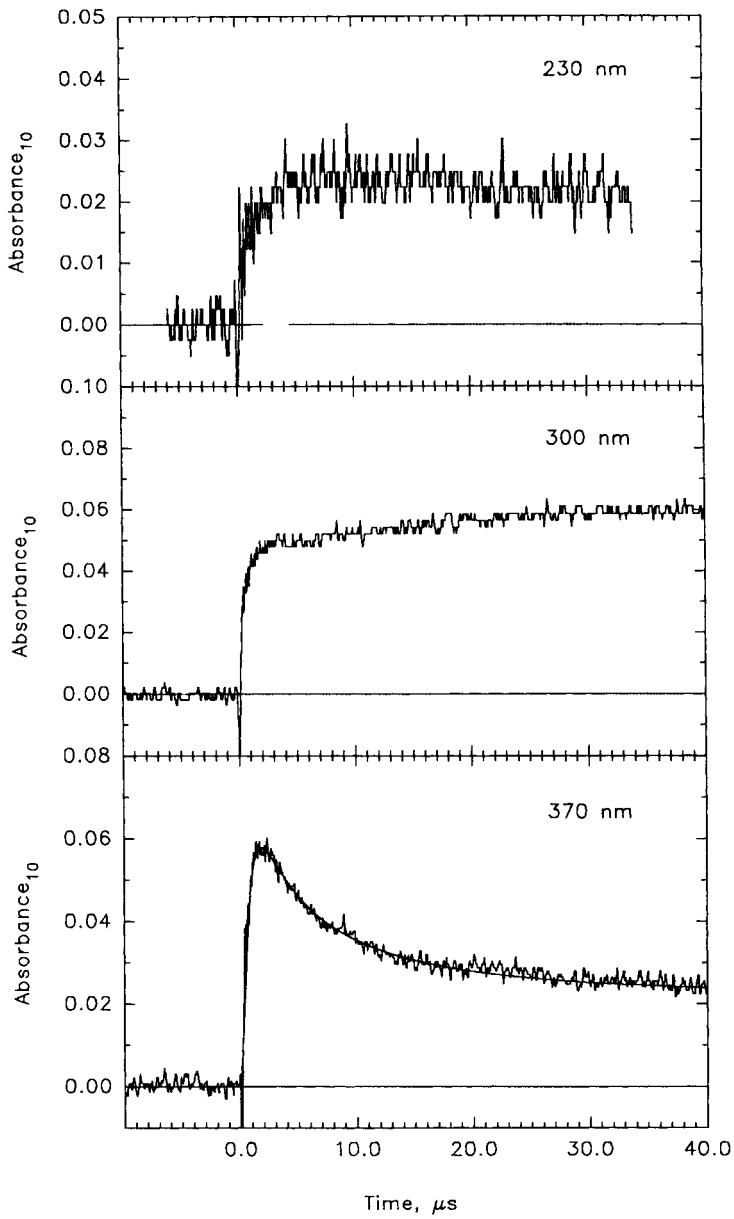

Figure 8. The transient UV absorption at 230 nm, 300 nm, and 370 nm following pulse radiolysis of mixtures of 1 mbar CH_3I, 40 mbar O_2, and 959 mbar SF_6.

peroxy radical self reactions, and the reciprocal of the decay half-life observed at 370 nm is proportional to the dose, a characteristic of second-order kinetics. If the reaction rate constants for reaction (14) and (15) are equal and secondary products do not influence the observed decay of CH_2IO_2 radicals significantly we end up with $k_{14} = k_{15} = 9 \times 10^{-11}$ cm^3 molecule^{-1} s^{-1}. k_{16} was taken to 3.7×10^{-13} cm^3 molecule^{-1} s^{-1} [2]. Since several assumptions had to be made to derive this value it should only be regarded as a rough estimate.

Discussion

The UV spectrum of CH_2I shown in Figure 5 contains two absorption maxima. The wavenumbers of the two CH_2I maxima are 35700 cm^{-1} and 43500 cm^{-1}. The energy difference between the maxima is so large that the two bands probably belong to different electronic transitions. Assignment of the electronic transitions requires detailed theoretical calculations which is beyond the scope of this work.

The CH_2IO_2 spectrum displayed in Figure 7 is compared to the spectra of CH_2FO_2, CH_2ClO_2, and CH_2BrO_2. The figure shows that the CH_2IO_2 spectrum is an unusual peroxy spectrum. The reason for this is not known to us, but it should be noted that the $CH_3COCH_2O_2$ spectrum has a similar shape [22]. The spectra of CH_2IO_2 and $CH_3COCH_2O_2$ might be explained by the presence of the usual terminal —O—O group and an additional absorbing chromophore, e.g., the I atom and the C═══O group, respectively.

The kinetics of CH_2I and CH_2IO_2 radicals observed in our system were complex because CH_2I and CH_2IO_2 were only produced in 36% yield and because our reaction mixture contained several absorbing species. The rate constants of the self reactions of CH_2I and CH_2IO_2 radicals could only be obtained from our experimental data after several assumptions had been made. In the CH_3I/SF_6 system IF, CH_2I, and CH_3 could be observed separately. Since our kinetic model fitted the kinetic behavior of all three species well and the assumptions seems reasonable from a general kinetic viewpoint, we believe the estimated rate constants are close to the true rate constants.

In the $CH_3I/O_2/SF_6$ system little information was available and the obtained rate constants are therefore very uncertain. However, the estimated rate constants, $k_{14} = k_{15} = 9.0 \times 10^{-11}$ cm^3 $molecule^{-1}$ s^{-1} appear to be the fastest observed for reaction between two peroxy radicals. A very fast decay of the CH_2IO_2 radicals is comparable to the very fast decay of CH_2BrO_2 radicals. The observed rate constant for the self-reaction of CH_2BrO_2 radicals is 3.3×10^{-11} cm^3 $molecule^{-1}$ s^{-1} [4]. In contrast the self-reaction rate constants for CH_2FO_2 and CH_2ClO_2 radicals are an order of magnitude lower [1,2].

As discussed in the introduction CH_2IO_2 radicals are of minor importance in the atmosphere. However, the untypical UV absorption spectrum of CH_2IO_2 radicals and the fast decay of CH_2IO_2 emphasizes that knowledge of UV absorption spectra, reactivity and decay mechanisms of peroxy radicals is far from complete. From properties of a homolog peroxy radical series like CH_2FO_2, CH_2ClO_2, CH_2BrO_2, and CH_2IO_2 it might be possible to find a structure dependence of peroxy radical properties. A correlation between peroxy radical structure and properties would be important. Prediction of reliable kinetic data of peroxy radicals which have not been studied previously would be an achievement for the tropospheric chemistry models. At present we have not been successful in finding a relationship between peroxy radical structure and kinetic behavior. Further work is therefore necessary to understand the properties of peroxy radicals.

Acknowledgment

JS would like to thank the Danish Research Academy for a research scholarship and OJN would like to thank the Commission of the European Communities for financial support.

Bibliography

[1] T. J. Wallington, P. Dagaut, and M. J. Kurylo, *Chem. Rev.*, **92,** 667 (1992).
[2] P. D. Lightfoot, R. A. Cox, J. N. Crowly, M. Destriau, G. D. Hayman, M. E. Jenkin, G. K. Moortgat, and F. Zabel, *Atmos. Environ.*, **26A,** 1805 (1992).
[3] T. J. Wallington, J. C. Ball, O. J. Nielsen, and E. Bartkiewicz, *J. Phys. Chem.*, **96,** 1241 (1992).
[4] O. J. Nielsen, J. Munk, G. Locke, and T. J. Wallington, *J. Phys. Chem.*, **95,** 8714 (1991).
[5] P. Dagaut, T. J. Wallington, and M. J. Kurylo, *Int. J. Chem. Kinet.*, **20,** 815 (1988).
[6] W. L. Chameides and D. D. Davis, *J. Geophys. Res.*, **85,** 7383 (1980).
[7] A. C. Brown, C. E. Canosa-Mas, and R. P. Wayne, *Atmos. Environ.*, **24A,** 361 (1990).
[8] R. P. Wayne, I. Barnes, P. Biggs, J. P. Burrows, C. E. Canosa-mas, J. Hjort, G. Le Bras, G. K. Moortgat, D. Perner, G. Restelli, and H. Sidebottom, *The Nitrate Radical: Physics, Chemistry and the Atmosphere,* 1990.
[9] K. B. Hansen, R. Wilbrandt, and P. Pagsberg, *Rev. Sci. Instrum.*, **50,** 1532 (1979).
[10] O. J. Nielsen, Risø-R-480, Risø National Laboratory, Roskilde, Denmark, 1984.
[11] T. Ellermann, Risø-M-2932, Risø National Laboratory, Roskilde, Denmark, 1991.
[12] T. Macpherson, M. J. Pilling, and M. J. C. Smith, *J. Chem. Phys.*, **89,** 2268 (1985).
[13] U. Wörsdörfer and H. Heydtmann, *Ber. Bunsenges. Phys. Chem.*, **93,** 1132 (1989).
[14] B. K. Clark and I. M. Littlewood, *Chem. Phys.*, **107,** 97 (1986).
[15] D. J. Bernard, M. A. Chawdbury, B. K. Winther, T. A. Seder, and H. H. Michels, *J. Phys. Chem.*, **94,** 7507 (1990).
[16] R. A. Durie, *Can. J. Phys.*, **44,** 337 (1966).
[17] D. Porret and C. F. Goodeve, *Proc. Roy. Soc., London Ser. A.*, **165,** 31 (1937).
[18] NIST Chemical Kinetics Data Base, Version 4.0.
[19] P. B. Roussel, P. D. Lightfoot, F. Caralp, V. Calone, R. Lesclaux, and W. Forst, *J. Chem. Soc. Faraday Trans.*, **87,** 2367 (1991).
[20] K. Sugawara, F. Ito, T. Nakanaga, H. Takeo, and C. Matsumura, *J. Chem. Phys.*, **92,** 5328 (1990).
[21] T. Ellermann, J. Sehested, O. J. Nielsen, P. Pagsberg, and T. L. Wallington, *Chem. Phys. Lett.*, submitted.
[22] R. A. Cox, J. Munk, O. J. Nielsen, P. Pagsberg, and E. Ratajczak, *Chem. Phys. Lett.*, **173,** 206 (1990).

Received April 29, 1993
Accepted July 12, 1993